Energy & Environmental Science

Accepted Manuscript

ROYAL SOCIETY OF CHEMISTRY

www.rsc.org/ees

Journal Name

RSCPublishing

COMMUNICATION

Enhancing Hydrogen Production of Microalgae by Redirecting Electrons from Photosystem I to Hydrogenase

Cite this: DOI: 10.1039/x0xx00000x

Received 00th May 2014,
Accepted 00th

DOI: 10.1039/x0xx00000x

www.rsc.org/

Sigrun Rumpel,*[a] Judith F. Siebel,[a] Christophe Farès,[b] Jifu Duan,[c] Edward Reijerse,[a] Thomas Happe,[c] Wolfgang Lubitz[a] and Martin Winkler*[c]

Photohydrogen generation in microalgae is catalysed by hydrogenases, which receive electrons from photosystem I via the ferredoxin PETF. The dominant acceptor of photosynthetic electrons is, however, the ferredoxin-NADP$^+$-oxidoreductase (FNR). By utilizing targeted ferredoxin and FNR variants in a light-dependent competition assay, electrons can be redirected to the hydrogenase yielding a five-fold enhanced hydrogen evolution activity.

INTRODUCTION

Dihydrogen (H_2) has the highest mass energy density of all known fuel types and as it can be generated from and converted back into water it is one of the most attractive energy carriers to appease both, the world's climate and energy crisis.[1, 2] The solar-driven bio-H_2 production by microalgae like *Chlamydomonas (C.) reinhardtii* complements chemical technologies for solar fuel generation.[3] Upon sulfur or nitrogen depletion *C. reinhardtii* switches to anaerobic growth conditions.[4-6] As a consequence of anaerobiosis, the [FeFe]-hydrogenase HYDA1 is expressed.[7] It receives electrons from photosystem I (PSI) via the plant-type photosynthetic electron transport ferredoxin (PETF) for catalysing the reversible reduction of protons to H_2.[8, 9] Under normal growth conditions PETF provides photosynthetic electrons for a variety of different metabolic pathways such as the assimilation of nitrate, sulfate and ammonia, as well as the reductive regeneration of glutathione. [10] Most of its electrons are, however, used for CO_2-fixation mediated by the PETF-dependent ferredoxin NADP$^+$ oxidoreductase (FNR) (Fig. 1).[11]

While [FeFe]-hydrogenases can achieve very high turnover rates of up to 10^4 molecules H_2 per second *in vitro*[12], H_2 evolution is strongly limited *in vivo* by the O_2 sensitivity of the hydrogenase[13] and the availability of reduced PETF.[14] The latter issue has been addressed in several studies demonstrating that through down-regulation of competing processes the electron flow of photosynthetic electrons can be redirected towards the hydrogenase HYDA1 inducing enhanced H_2 photoproduction.[15-18] Very recently it has been shown that a knock-down of FNR expression in *C. reinhardtii* leads to a 2.5-fold higher H_2-production activity under sulfur deprivation.[19] In another drastic approach Yacoby *et al.* were able to increase H_2 photoproduction using a PETF/HYDA1 fusion protein thus enforcing the bias of PETF to switch from FNR to HYDA1.[20]

However, for a stable photosynthetic growth a certain level of FNR activity has to be conserved and independent PETF is mandatory to dissipate at least a minor fraction of electrons to other essential redox pathways. In the long run a more subtle approach will be favored to develop a healthy growing algal strain with a strong but not self-destructive solitary focus on H_2 production.

In the current study, we follow a new approach at the molecular level aiming to reduce the PETF affinity for FNR without affecting its interaction with HYDA1. Both interactions are driven by Coulomb forces between conserved acidic PETF residues near the [2Fe-2S]-cluster with

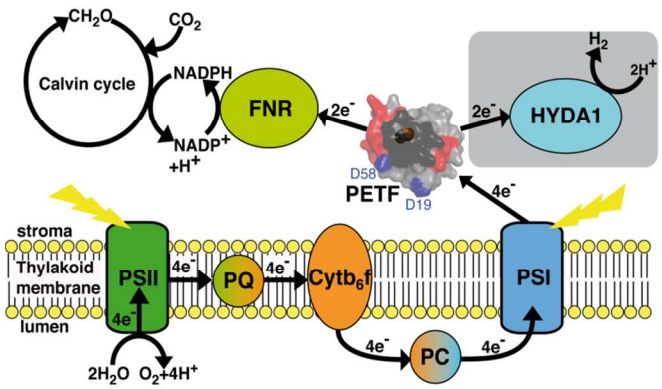

Fig. 1 Scheme showing competing electron transfer pathways in the chloroplast of the microalga *C. reinhardtii* leading either to H_2 or NADPH production. The surface presentation of PETF is shown with the residues closer than 7 Å to the [2Fe-2S]-cluster (black spheres) in dark grey. PETF residues affected by HYDA1-binding are coloured red (cf. Fig. 3). Residues D19 and D58 (see text) are in blue. H_2 production by HYDA1 requires anaerobic conditions (grey box). PSI and PSII, photosystems I and II, respectively; PQ, plastoquinone pool; PC, plastocyanine; Cyt, cytochrome.

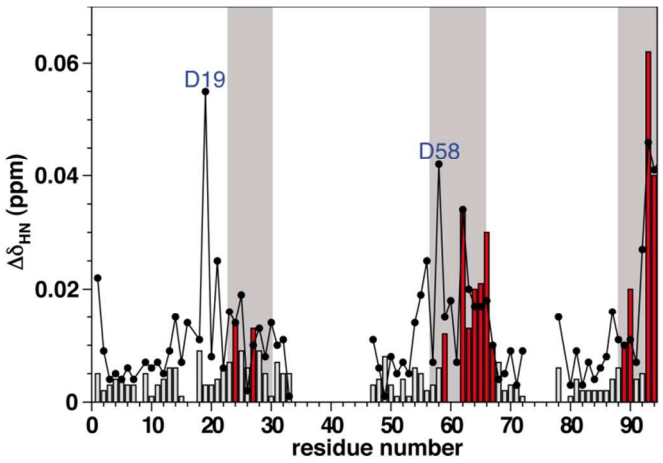

Fig. 3 NMR chemical shift perturbation of PETF upon complex formation with HYDA1 and FNR. Average backbone amide chemical shift changes ($\Delta\delta_{HN}$) for free and bound PETF at a 15-fold excess of HYDA1 (bars) and FNR (black line) were calculated according to the equation $\Delta\delta_{HN} = [(\Delta\delta_H^2 + 0.2\Delta\delta_N^2)/2]^{1/2}$ and plotted versus the residue number. Red bars indicate PETF residues with $\Delta\delta_{HN} \geq 0.01$ ppm upon HYDA1-binding. A grey background highlights the PETF regions known to bind to FNR (Table S1 in ESI†) which exhibit also the largest chemical shift changes upon complex formation with HYDA1 and FNR.

corresponding basic residues on HYDA1 and FNR. Many of the contact sites for the PETF/FNR interaction have already been identified using mutagenesis[21] and NMR-titration studies.[22, 23] The PETF/HYDA1 interaction has also been investigated based on mutagenesis studies.[9] These investigations were, however, not specifically aimed at a differentiation between the PETF/HYDA1 and PETF/FNR contacts.

Results and Discussion

To distinguish between contacts of PETF to HYDA1 and FNR, we conducted parallel NMR titrations of ^{15}N-labeled PETF with increasing amounts of HYDA1 or FNR and monitored the magnitude of the chemical shift changes ($\Delta\delta_{HN}$) of the backbone amide resonances of PETF using ^{1}H-^{15}N-TROSY-HSQC experiments (Fig. 2, see further details in ESI†).[24]

In addition, these residues are similar to the FNR-binding interfaces of highly homologous PETF molecules from other species (Table S1 in ESI†)[21, 22] and protrude to three directions from the [2Fe-2S]-cluster which is located close to one side of the molecular surface of PETF.[25] Overall, the observed chemical shift perturbations are small suggesting multiple orientations of the proteins in the complex, which have also been described for other electron transfer complexes like myoglobin/cytochrome b_5[26], cytochrome c/cytochrome b_5[27] and superoxide reductase/rubredoxin.[28] Importantly, when comparing the chemical shift changes for PETF/HYDA1 and PETF/FNR the two aspartate residues D19 and D58 can be identified as only affected upon FNR-binding (Figs. 2 and 3). The other residues, that are only significantly affected when FNR, but not when HYDA1 binds to PETF, are either not solvent accessible (Val54, Gln56, Thr87) or marginally affected in reduced

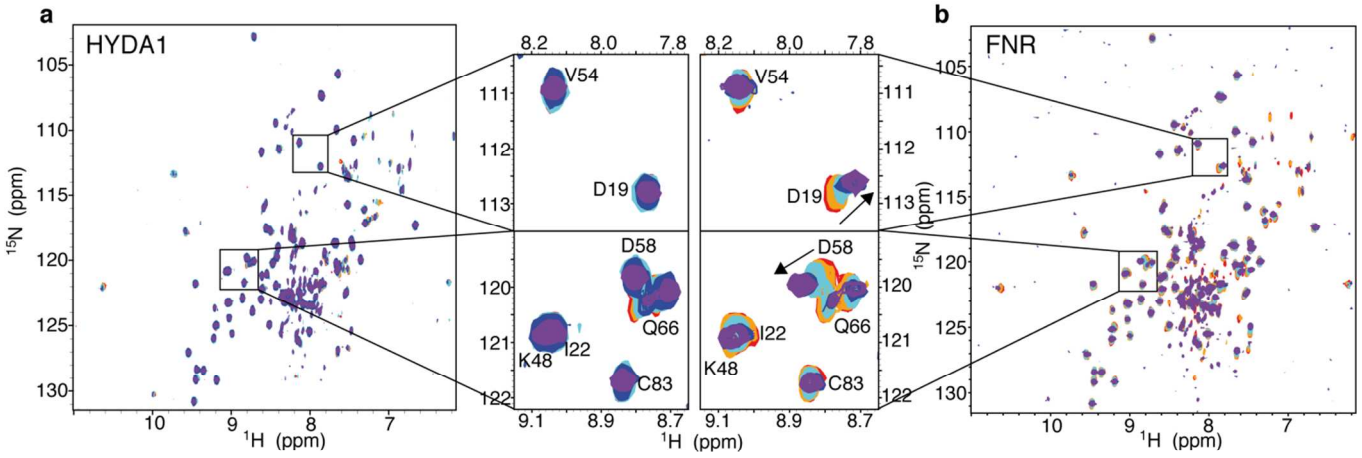

Fig. 2 NMR-titration analysis of the interaction of PETF with HYDA1 and FNR. Overlay of ^{1}H-^{15}N TROSY-HSQC spectra of PETF with HYDA1 (a) and FNR (b) at ratios of 1:0 (red), 1:1 (orange), 1:5 (cyan), 1:10 (blue) and 1:15 (violet). Backbone amide signals for residues 35-45 and 73-76 were not observed in the NMR-spectra due to a distance < 7 Å to the paramagnetic [2Fe-2S]-cluster.

In our study, the largest NMR chemical shift perturbations upon complex formation with HYDA1 and FNR were observed for the backbone amides of residues 23-28, 58-67 and 89-94 and, indeed, most identified PETF residues are involved in complex formations with both proteins (Fig. 3).

PETF (Tyr1, Tyr21, Asp55) (for further details see ESI†, Figs. S1-S3). The chemical shift changes indicate D58 as a part of the PETF-binding interface for FNR and as an immediate neighbor of the PETF-binding interface for HYDA1 (Fig. 3). Remarkably, D19 does not belong to the residues

surrounding the [2Fe-2S]-cluster (Fig. 1). A possible explanation for its importance is provided by the X-ray structure of the homologous PETF/FNR complex from *maize leaf*.[22] In this structure, D19 is about 12 Å away from the apparent N-terminal FNR residue, however, this structure is 18 and 13 amino acids shorter at the N-terminus compared to the native FNR of *maize leaf* and *C. reinhardtii,* respectively. These missing N-terminal residues might form an embracing loop with PETF and interact with D19 (Fig. S4 in ESI†). The identification of D19 and D58 of PETF as being solely important for the PETF/FNR and not for the PETF/HYDA1 complex suggests the differentiation between individual binding partners as a so far unknown function of the negatively charged residues of plant-type ferredoxins.

To investigate the potential use of D19 and D58 of PETF for improving bio-H_2 production their importance for differentiating between FNR and HYDA1 was confirmed by mutagenesis to alanine. The resulting three PETF variants (PETF-D19A, -D58A and -D19A/D58A) were examined in a light-driven H_2 production assay in absence and presence of FNR for their efficiency to donate electrons to HYDA1. This assay is a simplification of an earlier described reconstitution system[9] on the basis of proflavine (PF) as a photosensitizer substituting PSI. The original upstream electron transfer compounds 2,6-dichlorphenolindophenol and plastocyanine were omitted and instead of ascorbate a low concentration of EDTA was used as a sacrificial electron donor. To assess H_2 production by HYDA1 in direct competition with NADPH-production by FNR, equimolar concentrations of HYDA1 and FNR were used. The FNR co-substrate $NADP^+$ was further included alongside with the enzyme nitrate reductase from *Aspergillus niger*[29] to ensure a constant co-substrate recycling (Fig. 4, see further details in ESI†).

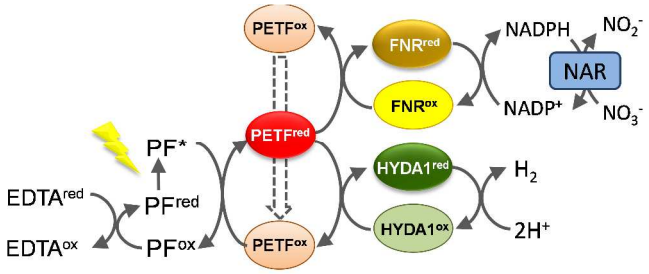

Fig. 4 Schematic illustration of the electron transfer pathway of the light-dependent H_2 production assay to investigate the competition between HYDA1 and FNR for reduced PETF. PF = proflavin; NAR = nitrate reductase; red = reduced; ox = oxidized.

In absence of FNR, the measured light-dependent HYDA1-activity remains almost unchanged for mutant-PETF when compared to wildtype (wt)-PETF (Fig. 5). However, in presence of FNR the H_2 production level of HYDA1 with wt-PETF is diminished to only 7% (Fig. 5) due to the significantly lower affinity of PETF for HYDA1 (21-35 µM)[9, 30] than for FNR (2.6-6.6 µM).[31] This HYDA1-activity is the control level of the competition assay, in which PETF-D19A exhibits an about 1.5-fold and PETF-D58A a 2.5-fold increased H_2 production (Fig. 5b). Importantly, H_2 production with PETF-D19A/D58A is even 4-fold increased indicating a synergistic enhancement of the single effects (Fig. 5b). These results confirm the role of the acidic PETF residues D19 and D58 for distinguishing HYDA1 and FNR. The high homology between plant-type [2Fe-2S]-ferredoxins from different origins (Fig. S5 in ESI†) further suggests a general importance of residues D19 and D58 to direct electrons towards FNR. Apart from that, PETF-D19A/D58A promises to be valuable for the bioengineering of an efficient H_2 production pathway.

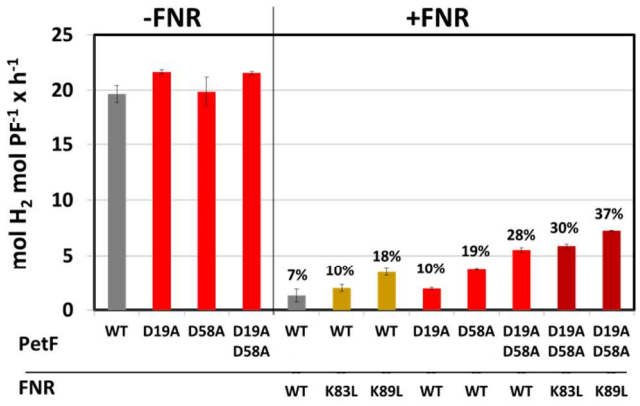

Fig. 5 Rates of light-dependent H_2 production determined for HYDA1 with wt- or mutant-PETF in absence (-FNR) and in presence of wt- or mutant-FNR (+FNR). The indicated 7% HYDA1-activity in presence of FNR refers to 100% HYDA1-activity in absence of FNR. Error bars depict the standard deviation of 4 independent measurements.

The profound shift of electron transfer away from FNR towards HYDA1 is even more pronounced when FNR variants are used that exhibit a decreased PETF-dependent catalytic efficiency.[31] The two FNR variants which have been earlier described to be affected either in the PETF affinity (FNR-K83L) or in the PETF-dependent maximum reaction rate (FNR-K89L) were assayed in comparison to wt-PETF (Fig. 5). FNR-K83L and -K89L allow for H_2 production rates about 1.5- and more than 2.5-fold higher than the control level, resembling the effects of PETF mutagenesis. Importantly, H_2 production is increased about 5-fold compared to the control level when performing the assay with FNR-K89L and PETF-D19A/D58A (Fig. 5b). This almost additive effect demonstrates that the electron transfer hierarchy can be most effectively shifted by addressing both, FNR and PETF.

We also examined PETF-D19A/D58A in the light-dependent H_2 production assay with PSI, which is the native electron donor for PETF and hence mimics more closely the *in vivo* situation in *C. reinhardtii*. In this PSI-dependent assay, light-driven H_2 production is slightly decreased for PETF-D19A/D58A in absence of FNR (Fig. 6) indicating that at least one exchange slightly affects the interaction with PSI. Nevertheless, the H_2 production activity in presence of FNR is increased about 3-fold for PETF-D19A/D58A compared to wt-PETF (Fig. 6) reproducing the result of the proflavin-dependent assay.

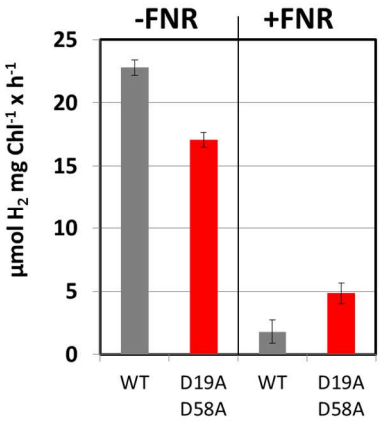

Fig. 6 PSI-dependent H2 photoproduction rates of HYDA1 with wt-PETF and PETF-D19A/D58A in absence (-FNR) and presence of FNR (+FNR). Error bars depict the standard deviation of 3-4 independent measurements.

Our knowledge-based variant PETF-D19A/D58A may be used in addition to or as part of a PETF/HYDA1 fusion protein as published by Yacoby *et al.* [20] to achieve the best H_2 production capacities. Furthermore, an implementation

of these modifications within a *C. reinhardtii* strain like *Stm6* with an about 5-fold higher H_2 evolution yield[16] is a promising strategy to increase the efficiency of microalgal H_2 production beyond the 5% light energy-to-H_2 conversion efficiency which is expected to be required for a commercial use.[32]

CONCLUSIONS

Conserved PETF aspartic acid residues D19 and D58 are crucial for the differential recognition of FNR and HYDA1 as electron transfer binding partner. Mutation of these residues to alanine suppresses FNR binding and redirects PETF electron flow towards HydA1 thus enhancing *in vivo* hydrogen production. It can be anticipated that also in other metabolic pathways highly conserved acidic ferredoxin residues are relevant for molecular recognition of its binding partners. The effects of PETF and FNR genetic modifications are additive,, i.e. the interaction efficiency of PETF for FNR can be further reduced by employing targeted FNR-K89L variants in combination with PETF-D19A/D58A variants. This combined metabolic engineering approach opens new avenues for the design of H_2-producing organisms with an increased photofermentative H_2 production.

MATERIALS AND METHODS

Protein preparation

All FeS-cluster containing proteins were heterologously expressed in *Escherichia coli* BL21(DE3)ΔiscR[33]. Recombinant HYDA1 holoprotein and PETF from *C. reinhardtii* were expressed and prepared as described earlier.[9, 34] Site directed exchanges were introduced following the QuikChange procedure described for the site-directed mutagenesis kit from Stratagene (Agilent Technologies). Introduced mutations were confirmed by DNA sequencing (3130x Genetic Analyzer, Applied Biosystems). The *fnr* cDNA of *C. reinhardtii* was amplified excluding the N-terminal sequence part that covers the chloroplast transit peptide[35] and cloned behind the Strep-tag II sequence of expression vector pASK-IBA7 (IBA GmbH, Goettingen). FNR was expressed in E. coli BL21(DE3)pLysS using lysogeny broth (LB) medium and purified analogously to PETF. Protein purity was verified via SDS-PAGE and Coomassie staining (Fig. S6).

Samples for NMR spectroscopy were expressed using E. coli codon optimized genes of *C. reinhardtii* PETF and HYDA1 inserted into pET21b. The expression plasmid for PETF contained a C- terminal TEV cleavage site preceded by a Strep-tag II and the expression plasmid for HYDA1 contained a N-terminal TEV cleavage site followed by a Strep-tag II. To prepare ^{15}N- and $^{13}C/^{15}N$-labeled samples, *E. coli* cells were grown in M9-based minimal medium containing $^{15}NH_4Cl$ and/or $^{13}C_6$-glucose. For purification, following affinity chromatography, the protein was incubated with TEV protease at a ratio of 1:1 (w/w) overnight at room temperature to remove the Strep-tag. The plasmid for expressing TEV protease was a gift of the Arrowsmith lab. The His6-tagged TEV protease was removed with Talon beads (Clontech) and PETF was further purified by gel filtration using a Superdex 75 16/60 (GE Healthcare). Recombinant apo-HYDA1 was activated by adding of $[Fe_2(CO)_4(CN)_2[(SCH_2)_2NH]]^{2-}$.

NMR spectroscopy

NMR samples contained 0.1-1 mM PETF in 50 mM potassium phosphate pH 6.8, 50 mM NaCl and 10% D_2O (v/v). All NMR experiments were acquired at 298 K on a Bruker AVANCE 600 spectrometer equipped with a cryogenic probehead. The 3D spectra employed a non-uniform sampling scheme in the indirect dimension und were reconstructed by the multi-dimensional decomposition software MDDNMR[36] interfaced with the MDDGUI[37] and NMRPipe/NMRDraw[38]. Backbone assignments were obtained using standard triple resonance experiments[39]. All spectra were analyzed using Sparky (T. D. Goddard and D. G. Kneller, University of California, San Francisco).

NMR titration experiments

PETF complex formation with HYDA1 and FNR was monitored by recording a series of 2D ^1H-^{15}N-TROSY-HSQC experiments of a 100 µM ^{15}N-labeled PETF solution with binding partner at a molar ratio of 1:0, 1:1, 1:2, 1:5, 1:10 and 1:15. Weighted averages of the ^1H and ^{15}N backbone chemical shift changes of a particular residue were calculated according to the equation $\Delta\delta_{HN} = [(\Delta\delta_H^2 + 0.2\Delta\delta_N^2)/2]^{1/2}$

Measurement of light-driven hydrogen production and competition assay

To determine the light-driven H_2 production, 50 nM HYDA1 was combined with wild type (wt) or mutant forms of 20 µM PETF. The total volume of 200 µl contained 40 mM EDTA (ethylene-diaminetetraacetic acid) as sacrificial electron donor and 200 µM proflavine (acridine-3,6-diamine) as a photosensitizer in 100 mM potassium phosphate pH 6.8, supplemented with 1 mM sodium dithionite and 3 mM $NaNO_3$.

To determine the H_2-production efficiency of HYDA1 under competitive conditions, 50 nM FNR and 2 mM $NADP^+$ were added. For stabilizing the level of $NADP^+$ and thus the competitive efficiency of the FNR during the H_2-production period, 0.36 U of nitrate reductase (NAR) from *Aspergillus niger* (Sigma-Aldrich) was further included. Compound concentrations were adjusted for optimal H_2-production efficiency (Fig. S7).

PSI-dependent H_2-photoproduction was measured as described earlier[30]. The assay comprised 5 mM sodium ascorbate, 0.6 mM DCPIP (2,6-Dichlorphenol-indophenol), 30 µM plastocyanin, 20 µM PETF, 50 nM HYDA1 in 20 mM Tris pH 7.4, 20 mM $MgCl_2$, 0.03% ß-DM, 1 mM sodium dithionite and 3 mM $NaNO_3$. PSI was added corresponding to the amount of 5 µg chlorophyll (Chl). For determining the PSI-dependent HYDA1-activity under competitive conditions 50 nM FNR, 2 mM $NADP^+$ and 0.036 U NAR were added.

All reaction samples were prepared under anoxic conditions in 2 ml Eppendorf tubes and sealed with Suba-Seal stoppers (size 13, Sigma-Aldrich). After sparging the reaction mixture with argon for 5 min, the reaction tubes were light-exposed (1200 µmol photons m^{-2} s^{-1}) under constant shaking at 37 °C. H_2-production was determined after 30 min by analyzing 400 µl of the head-space via gas chromatography (GC-2010, Shimadzu).

Acknowledgments

We thank Katharina Weber for providing $[Fe_2(CO)_4(CN)_2[(SCH_2)_2NH]]^{2-}$. This work was supported by the Max Planck Society and the Bundesministerium für Bildung und Forschung (BMBF) (Bio-H2) (to T.H. and W.L.). T.H. gratefully acknowledges support from the Deutsche Forschungsgemeinschaft (HA 255/2-1) and the Volkswagen Foundation (LigH2t).

Notes and references

[a] Max-Planck-Institut für Chemische Energiekonversion, Stiftstrasse 34-36, 45470 Mülheim an der Ruhr, Germany.
[b] Max-Planck-Institut für Kohlenforschung, Kaiser-Wilhelm-Platz 1, 45470 Mülheim an der Ruhr, Germany.
[c] Ruhr-Universität Bochum, Fakultät für Biologie und Biotechnologie, Lehrstuhl für Biochemie der Pflanzen, AG Photobiotechnologie, 44801 Bochum, Germany.

† Electronic Supplementary Information (ESI) available: [Experimental details and additional figures]. See DOI: 10.1039/c000000x/

1. J. Hetland and G. Mulder, *Int. J. Hydrogen Energy*, 2007, **32**, 736-747.
2. M. Ball and W. M., *Int. J. Hydrogen Energy*, 2009, **34**, 615-627.
3. A. Volgusheva, S. Styring and F. Mamedov, *Proc. Natl. Acad. Sci. U. S. A.*, 2013, **110**, 7223-7228.
4. A. Melis and T. Happe, *Plant Physiol.*, 2001, **127**, 740-748.

5. A. Melis, L. Zhang, M. Forestier, M. L. Ghirardi and M. Seibert, *Plant Physiol.*, 2000, **122**, 127-136.
6. G. Philipps, T. Happe and A. Hemschemeier, *Planta*, 2012, **235**, 729-745.
7. M. Pape, C. Lambertz, T. Happe and A. Hemschemeier, *Plant Physiol.*, 2012, **159**, 1700-1712.
8. S. T. Stripp and T. Happe, *Dalton Trans.*, 2009, 9960-9969.
9. M. Winkler, S. Kuhlgert, M. Hippler and T. Happe, *J. Biol. Chem.*, 2009, **284**, 36620-36627.
10. M. Winkler, A. Hemschemeier, J. Jacobs, S. Stripp and T. Happe, *Eur. J. Cell Biol.*
11. N. Carrillo and E. A. Ceccarelli, *Eur. J. Biochem.*, 2003, **270**, 1900-1915.
12. W. Lubitz, H. Ogata, O. Rudiger and E. Reijerse, *Chem. Rev.*, 2014, **114**, 4081-4148.
13. S. T. Stripp, G. Goldet, C. Brandmayr, O. Sanganas, K. A. Vincent, M. Haumann, F. A. Armstrong and T. Happe, *Proc. Natl. Acad. Sci. U. S. A.*, 2009, **106**, 17331-17336.
14. M. Winkler, S. Kawelke and T. Happe, *Bioresour Technol*, 2011, **102**, 8493-8500.
15. C. M. Agapakis, D. C. Ducat, P. M. Boyle, E. H. Wintermute, J. C. Way and P. A. Silver, *J. Biol. Eng.*, 2010, **4**, 3.
16. O. Kruse, J. Rupprecht, K. P. Bader, S. Thomas-Hall, P. M. Schenk, G. Finazzi and B. Hankamer, *J. Biol. Chem.*, 2005, **280**, 34170-34177.
17. T. Rühle, A. Hemschemeier, A. Melis and T. Happe, *BMC Plant Biol.*, 2008, **8**, 107.
18. D. Tolleter, B. Ghysels, J. Alric, D. Petroutsos, I. Tolstygina, D. Krawietz, T. Happe, P. Auroy, J. M. Adriano, A. Beyly, S. Cuine, J. Plet, I. M. Reiter, B. Genty, L. Cournac, M. Hippler and G. Peltier, *Plant Cell*, 2011, **23**, 2619-2630.
19. Y. Sun, M. Chen, H. Yang, J. Zhang, T. Kuang and F. Huang, *Int. J. Hydrogen Energy*, 2013, **38**, 16029-16037.
20. I. Yacoby, S. Pochekailov, H. Toporik, M. L. Ghirardi, P. W. King and S. Zhang, *Proc. Natl. Acad. Sci. U. S. A.*, 2011, **108**, 9396-9401.
21. T. Mayoral, M. Martinez-Julvez, I. Perez-Dorado, J. Sanz-Aparicio, C. Gomez-Moreno, M. Medina and J. A. Hermoso, *Proteins*, 2005, **59**, 592-602.
22. G. Kurisu, M. Kusunoki, E. Katoh, T. Yamazaki, K. Teshima, Y. Onda, Y. Kimata-Ariga and T. Hase, *Nat. Struct. Biol.*, 2001, **8**, 117-121.
23. P. N. Palma, B. Lagoutte, L. Krippahl, J. J. G. Moura and F. Guerlesquin, *FEBS Lett.*, 2005, **579**, 4585-4590.
24. K. Pervushin, R. Riek, G. Wider and K. Wuthrich, *Proc. Natl. Acad. Sci. U. S. A.*, 1997, **94**, 12366-12371.
25. K. Fukuyama, *Photosynthesis Research*, 2004, **81**, 289-301.
26. J. A. R. Worrall, Y. Liu, P. B. Crowley, J. M. Nocek, B. M. Hoffman and M. Ubbink, *Biochemistry*, 2002, **41**, 11721-11730.
27. A. N. Volkov, D. Ferrari, J. A. R. Worrall, A. M. J. J. Bonvin and M. Ubbink, *Protein Sci.*, 2005, **14**, 799-811.
28. R. M. Almeida, P. Turano, I. Moura, J. J. Moura and S. R. Pauleta, *Chembiochem*, 2013, **14**, 1858-1866.
29. B. Dziedzic, J. Mazanowska-Gajdowicz, A. Walczewska, A. Sarniak and D. Nowak, *Clin. Chim. Acta*, 2003, **335**, 65-74.
30. T. Happe and J. D. Naber, *Eur. J. Biochem.*, 1993, **214**, 475-481.
31. P. Decottignies, V. Flesch, C. Gerard-Hirne and P. Le Marechal, *Plant Physiol. Biochem.*, 2003, **41**, 637-642.
32. E. Stephens, I. L. Ross, Z. King, J. H. Mussgnug, O. Kruse, C. Posten, M. A. Borowitzka and B. Hankamer, *Nat. Biotechnol.*, 2010, **28**, 126-128.
33. M. K. Akhtar and P. R. Jones, *Appl. Microbiol. Biotechnol.*, 2008, **78**, 853-862.
34. J. Esselborn, C. Lambertz, A. Adamska-Venkatesh, T. Simmons, G. Berggren, J. Noth, J. Siebel, A. Hemschemeier, V. Artero, E. Reijerse, M. Fontecave, W. Lubitz and T. Happe, *Nat. Chem. Biol.*, 2013, **9**, 607-609.
35. P. Decottignies, P. Lemarechal, J. P. Jacquot, J. M. Schmitter and P. Gadal, *Arch. Biochem. Biophys.*, 1995, **316**, 249-259.
36. A. Gutmanas, P. Jarvoll, V. Y. Orekhov and M. Billeter, *J. Biomol. NMR*, 2002, **24**, 191-201.
37. A. Lemak, A. Gutmanas, S. Chitayat, M. Karra, C. Fares, M. Sunnerhagen and C. H. Arrowsmith, *J. Biomol. NMR*, 2011, **49**, 27-38.
38. F. Delaglio, S. Grzesiek, G. W. Vuister, G. Zhu, J. Pfeifer and A. Bax, *J. Biomol. NMR*, 1995, **6**, 277-293.
39. A. Bax and S. Grzesiek, *Acc. Chem. Res.*, 1993, **26**, 131-138.

Broader context

The most urgent challenge of our time is to replace the dwindling resources of fossil fuels by sustainable non-polluting alternatives. Hydrogen is a promising energy vector and can be utilized as a regenerative carrier of emission-free energy especially when produced photo-biologically. Unicellular green algae like *Chlamydomonas reinhardtii* are known to produce hydrogen light-dependently. Their highly efficient [FeFe]-hydrogenase (HYDA1) catalyzes the reversible reduction of protons and electrons to dihydrogen. However, evolutionary and physiological constraints severely restrict the hydrogen yield of algae. An important key to achieve an economically viable biohydrogen production is the understanding and modulation of the photosynthetic electron flow via the ferredoxin PETF to HYDA1 which is limited by its competition with enzymes of other metabolic pathways. The most important alternative electron transfer pathway results in NADPH production by the ferredoxin/NADP+-oxidoreductase (FNR). Here, we were able to identify targets for manipulating the common redox-partner binding site of PETF to selectively shift the bias of PETF from FNR towards HYDA1. Indeed, genetic modifications of the identified residues result in an enhanced light-driven hydrogen production and might lead to the design of an economically competitive hydrogen producing organism.